

The Discovery of Water Maser Emission from Eight Nearby Galaxies

J.A. Braatz

National Radio Astronomy Observatory, 520 Edgemont Rd., Charlottesville, VA 22903

`jbraatz@nrao.edu`

and

N.E. Gugliucci

Department of Astronomy, University of Virginia, Charlottesville, VA 22904

`neg9j@virginia.edu`

ABSTRACT

Using the Green Bank Telescope, we conducted a “snapshot” survey for water maser emission toward the nuclei of 611 galaxies and detected eight new sources. The sample consisted of nearby ($v < 5000 \text{ km s}^{-1}$) and luminous ($M_B < -19.5$) galaxies, some with known nuclear activity but most not previously known to host AGNs. Our detections include both megamasers associated with AGNs and relatively low luminosity masers probably associated with star formation. The detection in UGC 3789 is particularly intriguing because the spectrum shows both systemic and high-velocity lines indicative of emission from an AGN accretion disk seen edge-on. Based on six months of monitoring, we detected accelerations among the systemic features ranging from 2 to $8 \text{ km s}^{-1} \text{ yr}^{-1}$, the larger values belonging to the most redshifted systemic components. High-velocity maser lines in UGC 3789 show no detectable drift over the same period. Although UGC 3789 was not known to be an AGN prior to this survey, the presence of a disk maser is strong evidence for nuclear activity, and an optical spectrum obtained later has confirmed it. With follow up observations, it may be possible to measure a geometric distance to UGC 3789.

Subject headings: galaxies: active — galaxies: nuclei — galaxies: Seyfert — ISM: molecules — masers — radio lines: galaxies

1. Introduction

Water maser emission at 22 GHz is commonly detected toward Galactic H II regions, pinpointing the locations of massive star formation. The median isotropic line luminosity in these sources is $10^{-4} L_{\odot}$ (Genzel & Downes, 1977), although in exceptional cases such as W49 the luminosity can reach $\sim 1 L_{\odot}$. Analogs to the W49 maser have been observed in H II regions of several nearby galaxies as well, where the combined radiation from multiple sites of star formation can lead to somewhat larger luminosities. The most distant (14.5 Mpc) and luminous ($L_{H_2O} \sim 8 L_{\odot}$) example of this type was detected toward the starburst galaxy NGC 2146 (Tarchi et al. 2002). In recent years, masers in extragalactic star-forming regions have become an important tool for measuring proper motions of the host galaxies, as in IC 10 and M 33 (Brunthaler et al. 2005, 2007)

Extragalactic water masers are also detected toward some active galactic nuclei (AGN), usually Seyfert 2 or LINER galaxies (Braatz et al. 1997). These sources have been called “megamasers” because the isotropic line luminosities exceed the median value of Galactic masers by ~ 6 orders of magnitude. Both galactic and extragalactic masers, however, are not believed to emit isotropically so the true line luminosity is smaller in each case by an unknown beaming factor. Masers in AGN accretion disks, specifically, are thought to be beamed in the plane of the disk.

High resolution imaging shows that megamasers are located within parsecs of the galactic nucleus, where they are associated either with jet-cloud interactions, nuclear outflows, or parsec-scale accretion disks. Unlike star formation masers, which only have Doppler components detected within $\sim 200 \text{ km s}^{-1}$ of the galaxy systemic recession velocity, masers in AGN accretion disks have shown velocity offsets up to $\sim 1300 \text{ km s}^{-1}$ (Kondratko et al. 2006a) owing to rotation about the central black hole. In the case of NGC 4258, masers trace the accretion disk 0.11 – 0.28 pc from the black hole (Argon et al. 2007), and have been used to measure the most precise geometric distance to a galaxy, 7.2 ± 0.2 (random statistical) ± 0.5 (systematic) Mpc (Herrnstein et al. 1999). The topic of extragalactic masers has recently been reviewed by Lo (2005).

NGC 4258 is currently the only galaxy with a robust maser distance, but large surveys are seeking additional examples of disk masers appropriate for such a measurement. Most surveys target Seyfert 2 and LINER galaxies (e.g. Greenhill et al. 2003; Braatz et al. 2004; Kondratko et al. 2006a, 2006b). With sensitive observations using large aperture telescopes, overall detection rates are $\sim 5\%$, and several disk masers have been identified. The masers detected by these surveys tend to be faint (peak fluxes of a few tens of mJy) and challenging to study in detail. Candidates for new surveys are limited by the number of AGNs identified in optical surveys.

While disk masers are clearly associated with active galaxies, the luminosity of the host AGN is modest in several of the most interesting cases. For example, the bolometric luminosity of NGC 4258, which has been classified either as a LINER or a weakly active Sy 1.9, is only 10^{42} erg s $^{-1}$ (e.g. Chary et al. 2000). Furthermore, Ho et al. (1997) found that 43% of a magnitude-limited sample of nearby galaxies host AGN, mostly with low luminosity, demonstrating that many apparently normal galaxies in fact host low luminosity AGN. We were thus motivated to conduct a new survey for H $_2$ O maser emission in nearby galaxies not necessarily known to host AGNs. Our intention was to identify bright maser systems ($\gtrsim 50$ mJy) conducive to detailed Very Long Baseline Interferometry (VLBI) imaging and spectral line monitoring. With the GBT we can identify such masers using short integrations, making it possible to observe a large sample and balance the relatively low detection rate expected.

2. Observations

We conducted observations between 2005 September 27 and 2007 April 14 using the Green Bank Telescope (GBT) of the National Radio Astronomy Observatory. The project was observed in 31 individual sessions, often assigned to fill short gaps in the telescope schedule. We configured the spectrometer with two 200 MHz spectral windows, each with 8192 channels, giving a channel spacing of 24 kHz corresponding to 0.33 km s $^{-1}$ at 22 GHz. The spectral windows were overlapped slightly such that the total bandwidth coverage was 380 MHz (5100 km s $^{-1}$). The systemic recession velocity of each galaxy was typically centered in one spectral window and the second window was offset to the red. For a few galaxies, the spectral windows were tuned with the systemic recession velocity in the overlap region, giving symmetric velocity coverage. We observed in dual circular polarization using a total power nodding mode in which the galaxy was placed alternately in one of two beams of the 18 – 22 GHz K-band receiver. A nodding cycle of 2.5 minutes per beam provided 5 minutes of integration per source. When time permitted, we obtained longer integrations to investigate possible detections.

We reduced and analyzed the data using GBTIDL. In order to enhance weak signals, we smoothed the blank sky reference spectra using a 16-channel boxcar function prior to calibration. We corrected the spectra for atmospheric attenuation using opacities derived from weather data, and we applied an elevation-dependent gain curve. The flux density scale uncertainty is about 15%, limited by noise tube calibration and pointing errors. To remove residual baseline shapes from each 200 MHz spectrum, we subtracted a polynomial (typically third order) fit to the line-free channels of the calibrated spectrum. Typical rms noise levels for the 5-minute observations were 6 mJy per 0.33 km s $^{-1}$ channel, after Hanning

smoothing.

Our candidate galaxies were selected from the Third Reference Catalog of Bright Galaxies (de Vaucouleurs et al. 1991) using coarse criteria intended primarily to eliminate galaxies without well-defined nuclei and those unlikely to host a hidden AGN. The sample has (1) systemic recession velocity $v < 5000 \text{ km s}^{-1}$, which corresponds to the distance at which the GBT could detect the NGC 4258 maser in 5 minutes; (2) Hubble stage $-3 < T < +5$ to choose lenticulars and early-type spirals; (3) absolute magnitude $M_B < -19.5$ to eliminate dwarf galaxies and boost the likelihood of a prominent nuclear black hole; and (4) declinations north of -30° , accessible to the GBT. We also eliminated galaxies previously searched with the GBT. These criteria identified 1074 candidate galaxies, not all of which were observed in the allotted time. We plan to observe the remaining galaxies in ongoing surveys. Galaxies were finally chosen for observation based on nearest neighbors, to minimize telescope slew time.

3. Results

We searched for 22 GHz H₂O maser emission toward the nuclei of 611 galaxies and detected masers in eight. Table 1 lists properties of the detected masers and Table 2 lists the undetected galaxies from the survey, along with relevant observing parameters. Each new maser was detected in more than one observing session except the one in NGC 1106, which was not identified until the data were reexamined at the conclusion of the scheduled observing. The best spectrum for each of the newly detected maser systems is shown in Figure 1. Velocities quoted in this paper are heliocentric and use the optical definition of Doppler shift.

Comments on the new masers and their host galaxies follow. For several of the galaxies, we discuss the maser profile in the context of an accretion disk maser. In this model, “systemic” emission refers to masers on the near side of the edge-on disk, along the line of sight to the black hole. “High-velocity” emission refers to masers located on the midline of the disk, rotating directly toward or away from the observer.

3.1. NGC 23

The maser detected in NGC 23 exhibits a broad profile relatively free of isolated, narrow features and centered near the systemic velocity (Figure 1). The spectrum shows no evidence of high-velocity lines. The isotropic luminosity of the source is $180 L_\odot$, suggesting the

maser is associated with an AGN. The profile resembles those from masers associated with nuclear jets, such as NGC 1052 (Claussen et al. 1998) and Mrk 348 (Peck et al. 2003). However, NGC 23 is not known to have an AGN. With $\log L_{IR} = 11.05 L_{\odot}$ (Sanders et al. 2003), NGC 23 is a luminous infrared galaxy (LIRG). The intense star formation associated with LIRGs might be expected to produce a large number of star-formation masers whose cumulative emission could reach the observed isotropic luminosity in NGC 23. However, Zhang et al. (2006) point out that the ultraluminous infrared galaxy (ULIRG) Arp 220 would have been detected easily in recent surveys if the maser emission were correlated with IR luminosity, yet Arp 220 has not been detected in H_2O . Two ULIRGs have been detected in the water maser line: UGC 5101 (Zhang et al. 2006) and NGC 6240 (Hagiwara et al. 2002; Nakai et al. 2002; Braatz et al. 2003). In both cases the masers appear to be associated with an AGN and not star formation (Hagiwara et al. 2003; Zhang et al. 2006). High resolution imaging could resolve the issue of whether the maser in NGC 23 is associated with star formation or an AGN.

3.2. NGC 1106

NGC 1106 is an emission line galaxy, called a Seyfert 2 by Bonatto et al. (1996). The maser detected in this galaxy contains a single, narrow (1.0 km s^{-1} FWHM) component at 3814 km s^{-1} , offset by 523 km s^{-1} from the 4337 km s^{-1} systemic recession velocity. The large velocity offset hints that the maser may be a high-velocity line in an accretion disk. The peak flux density is 74 mJy. Because the maser was not identified until all observations had been completed, we did not obtain a confirmation spectrum for this source. However, the maser line appears in both polarizations and in both beams of our observation. An observation of NGC 1106 by Kondratko et al. (2006b) with 13 mJy rms sensitivity failed to detect the line, but it would have appeared only at about 4σ given their channel spacing of 1.3 km s^{-1} . We also note that variability is common in narrow high-velocity lines.

3.3. UGC 3193

The maser observed toward the barred spiral galaxy UGC 3193 spans $\sim 350 \text{ km s}^{-1}$ and is localized in four distinct velocity windows. The profile shows remarkable symmetry about the galaxy’s recession velocity, even in the details of the inner two complexes. However, no lines are detected at the systemic velocity itself. The profile thus hints that the maser originates in a slowly rotating, edge-on disk, with only high-velocity features detected. A spiral density pattern in an accretion disk or discrete rings could produce a pattern as

observed. The absence of emission directly at the systemic velocity may indicate that the disk inclination or a warp prevents beaming of masers on the near side of the disk into our line of sight. Alternatively, a lack of background continuum emission that would otherwise provide seed emission for systemic features could account for the absence of detectable maser emission near the systemic velocity.

3.4. UGC 3789

The maser detected in UGC 3789 shows a profile characteristic of emission from an edge-on nuclear accretion disk. Maser lines are detected in three distinct velocity ranges (Figure 1), roughly symmetric about the galaxy’s recession velocity of $3325 \pm 24 \text{ km s}^{-1}$. Systemic lines are centered near 3275 km s^{-1} , offset slightly from the reported recession velocity. High velocity lines span $\sim 1500 \text{ km s}^{-1}$, suggesting the maser disk traces rotation speeds up to $\sim 750 \text{ km s}^{-1}$.

Upon associating the maser in UGC 3789 with disk emission, we initiated a program to observe the source at roughly 3-week intervals in order to track the velocities of systemic maser components and measure the centripetal acceleration of the maser gas in orbit around the central black hole. The initial results of this monitoring program are shown in Figures 2 and 3. With the six months of data presented here we have measured accelerations for nine individual lines among the systemic features. The accelerations, listed in the Figure 2 caption, range from $1.8 - 8.1 \text{ km s}^{-1} \text{ yr}^{-1}$, with the smallest accelerations measured near $\sim 3245 \text{ km s}^{-1}$ on the blue edge of the systemic features and the largest near $\sim 3310 \text{ km s}^{-1}$ on the red edge. The mean of the nine accelerations identified in Figure 2 is $4.0 \pm 0.8 \text{ km s}^{-1} \text{ yr}^{-1}$. The wide range of measured accelerations likely indicates that the systemic masers are not confined to a radially thin ring, but rather are spread over a range of radial distance from the dynamical center of the galaxy. The acceleration of systemic masers in NGC 4258 also varies for different components, although with a smaller range (e.g. Humphreys et al. 2008). Among the high-velocity features, measured accelerations are all less than $0.3 \text{ km s}^{-1} \text{ yr}^{-1}$. Additional monitoring observations of UGC 3789 and a more detailed analysis of the accelerations will follow in a later paper.

A robust measurement of the mass of a black hole can be made by measuring the rotation curve of a maser disk from a VLBI map. Without VLBI we can still make an estimate. If we suppose that the systemic masers with the largest measured acceleration occur at the same orbital radius as gas producing the largest rotation velocities among the high-velocity masers and that the accretion disk is edge-on, we can approximate M_{bh} , the mass of the black hole, by $M_{bh} = rv^2/G = v^4/aG$. Here r is the radius of the orbiting gas, v is its rotation velocity,

a is the centripetal acceleration, and G is the gravitational constant. Then $v \sim 750 \text{ km s}^{-1}$ and $a \sim 8.1 \text{ km s}^{-1} \text{ yr}^{-1}$ gives $M_{bh} \sim 9 \times 10^6 M_{\odot}$ for UGC 3789.

The systemic maser features in UGC 3789 are themselves split at $\sim 3275 \text{ km s}^{-1}$ by a dip in the emission (Figure 3). At times, the systemic emission in NGC 4258 has shown a similar dip (e.g. Greenhill et al. 1995a), although later data showed no evidence for it in that galaxy (Bragg et al. 2000). Watson & Wallin (1994) and Maoz & McKee (1998) developed models that invoke an absorbing layer of noninverted H_2O in the maser disk to account for a dip in the emission.

Megamaser emission is a beacon of nuclear activity. While UGC 3789 had not been identified as an AGN prior to our survey, an optical spectrum of the nucleus of the galaxy (Macri, private communication) reveals line flux ratios, such as $[\text{O III}]5007/\text{H}\beta$ and $[\text{O I}]6300/\text{H}\alpha$, and line widths of $\text{H}\alpha$ and $\text{H}\beta$ indicative of a Seyfert 2 nucleus.

With additional observations, it might be possible to measure the distance to UGC 3789 using the maser method applied to NGC 4258 (Herrnstein et al. 1999). We are continuing GBT monitoring and collecting sensitive VLBI observations for this purpose, and the results of these studies will be presented in later papers.

3.5. NGC 2989

The weak maser emission detected in NGC 2989 spans 30 km s^{-1} and is centered near the systemic recession velocity of the galaxy. No high velocity lines are detected. Although the isotropic luminosity ($40 L_{\odot}$) is large compared to masers in star formation regions, this galaxy has a nuclear H II region (Veron-Cetty & Veron, 2003) and the line profile is otherwise consistent with maser emission associated with star formation. If confirmed as a star formation maser, this galaxy, at a nominal distance of 58 Mpc (assuming $H_0 = 72 \text{ km s}^{-1} \text{ Mpc}^{-1}$) would be the most distant known source of such emission. However we cannot rule out the possibility that the maser is associated with an AGN.

3.6. NGC 3359

The maser emission from NGC 3359 has several weak, narrow features spanning $\sim 10 \text{ km s}^{-1}$ with a total isotropic luminosity of $0.7 L_{\odot}$, comparable to the luminosity of the strongest masers from H II regions in the Milky Way. No high-velocity lines are evident in the maser spectrum. NGC 3359 is an H II galaxy, and the maser is consistent with star formation.

3.7. NGC 4527

In addition to containing a LINER (Ho et al. 1997), the galaxy NGC 4527 is bright in the far infrared ($S_{100\mu m} = 64$ Jy; Fullmer & Lonsdale 1989). Such far-infrared emission is commonly associated with dust heated by young, massive stars. The galaxy has been searched for H₂O maser emission previously by Kondratko et al. (2006b) and Henkel et al. (2005) but went undetected. The rms sensitivities in their observations were 12 mJy per 1.3 km s⁻¹ channel and 15 mJy per 1.1 km s⁻¹ channel, respectively. The modest isotropic luminosity ($4 L_{\odot}$) is consistent with maser emission from a star formation region, but the velocity offset from the systemic recession velocity (170 km s⁻¹) leaves open the possibility that the maser is associated with the LINER. We note that NGC 4527 was host to the peculiar type Ia supernove 1991T.

3.8. NGC 7479

With a type 1.9 Seyfert nucleus (Ho et al. 1997), NGC 7479 has been targeted in previous surveys for H₂O masers in AGNs, including those by Kondratko et al. (2006b) and Braatz et al. (1996), in which the rms sensitivities were 19 mJy per 1.3 km s⁻¹ channel and 54 mJy per 0.66 km s⁻¹ channel, respectively. We detected the 140 mJy line at 2532 km s⁻¹ in the initial 5-minute integration, and the deeper spectrum shown in Figure 1 then revealed a number of distinct, weaker components redward of the systemic velocity. If the lines originate in an edge-on nuclear disk, the implied rotation speeds range up to 280 km s⁻¹.

4. Discussion

Megamasers in accretion disks can play an important role in cosmology. As a complement to observations of the cosmic microwave background, a precise ($\lesssim 3\%$) determination of the Hubble constant would provide a strong constraint on several key cosmological parameters, including the equation of state of dark energy (Hu 2005; Spergel et al. 2007). Measuring distances to water maser galaxies can contribute to improving the Hubble constant in two ways. First, maser distances to nearby galaxies ($D \lesssim 30$ Mpc) such as NGC 4258 can be used to refine the absolute calibration of Cepheid variables and replace or supplement the Large Magellanic Cloud as the primary anchor in the extragalactic distance scale (Macri et al. 2006). Second, maser distances to galaxies in the Hubble flow can be used to measure H_0 directly. Because maser distances are not based on standard candles and individual

uncertainties should be uncorrelated, it may be possible to reduce the total error in H_0 by measuring many such distances (e.g. Greenhill 2004). So far, however, a maser distance has only been possible for NGC 4258 (Herrnstein et al. 1999), and it is too close to measure H_0 directly.

Measuring maser distances to galaxies requires a robust model of the rotation structure and geometry of the accretion disk from VLBI imaging and either proper motions of maser features on the near side of the disk, or centripetal accelerations measured by spectral line monitoring. While proper motions ($\sim 30 \mu\text{as yr}^{-1}$ in NGC 4258 at 7.2 Mpc, Herrnstein et al. 1999) might be challenging for galaxies in the Hubble flow, measuring accelerations is possible, as demonstrated here for UGC 3789. We note, however, that in UGC 3789 additional monitoring will be necessary to properly model the radial structure implied by the variation in accelerations among different maser components.

Prospects for mapping and modeling the disk in UGC 3789 based on VLBI observations can only be assessed when that imaging is available. However, it is clear from the large number of bright ($\gtrsim 20$ mJy) maser features within each of the three spectral complexes that the rotation curve can be well sampled. Moreover, the mean acceleration ($\sim 4.0 \text{ km s}^{-1} \text{ yr}^{-1}$) and mean rotation velocity ($\sim 600 \text{ km s}^{-1}$) suggest a disk radius of ~ 0.09 pc. At a nominal distance to UGC 3789 of 46 Mpc, this corresponds to ~ 0.4 mas. Such a maser disk can be resolved by VLBI at 22 GHz.

5. Summary

In this survey for extragalactic water masers we employed a “snapshot” strategy designed to detect bright emission from nearby galaxies that may host hidden nuclear activity. Although the detection rate was low (1.3%) we observed a large number of galaxies and detected eight new masers. While it is not possible to assess the nature of these systems until they are imaged with interferometers, several appear particularly interesting. If confirmed as a star formation maser, the source in NGC 2989 would be the most distant and luminous example of that class. The maser in NGC 23 has a profile that resembles those of jet masers, but it is a LIRG and not known to host an AGN. In UGC 3193 the maser profile is remarkably symmetric but shows no emission directly at the systemic velocity of the galaxy. The most intriguing detection is in UGC 3789, which was not previously known to be an AGN. Its spectral profile is characteristic of maser emission from an accretion disk, and we have made a preliminary measurement of accelerations for several of its systemic features. With future VLBI studies and disk modeling, it may be possible to measure a geometric distance to this galaxy based on observations of its maser disk.

We thank Lucas Macri for providing an optical spectrum of UGC 3789. We are grateful for the many contributions from the NRAO staff in Green Bank. We also thank Jim Condon, Lincoln Greenhill, Mark Reid, Fred Lo, and Christian Henkel for useful discussions. The National Radio Astronomy Observatory is a facility of the National Science Foundation operated under cooperative agreement by Associated Universities, Inc. This research has made use of the NASA/IPAC Extragalactic Database (NED) which is operated by the Jet Propulsion Laboratory, California Institute of Technology, under contract with the National Aeronautics and Space Administration.

REFERENCES

- Argon, A.L., Greenhill, L.J., Reid, M.J., Moran, J.M. & Humphreys, E.M.L. 2007, *ApJ*, 659, 1040
- Barvainis, R. & Antonucci, R. 2005, *ApJ*, 628, L89
- Bonatto, C., Bica, E., Pastoriza, M.G. & Alloin, D. 1996, *A&AS*, 118, 89
- Braatz, J.A., Henkel, C., Greenhill, L.J., Moran, J.M. & Wilson, A.S. 2004, *ApJ*, 617, L29
- Braatz, J.A., Wilson, A.S., & Henkel, C. 1996, *ApJS*, 106, 51
- Braatz, J.A., Wilson, A.S., & Henkel, C. 1997, *ApJS*, 110, 321
- Braatz, J.A., Wilson, A.S., Henkel, C., Gough, R. & Sinclair, M. 2003, *ApJS*, 146, 249
- Bragg, A.E., Greenhill, L.J., Moran, J.M. & Henkel, C. 2000, *ApJ*, 535, 73
- Brunthaler, A., Reid, M.J., Falcke, H., Greenhill, L.J. & Henkel, C. 2005, *Science*, 307, 1440
- Brunthaler, A., Reid, M.J., Falcke, H., Henkel, C., & Menten, K.M. 2007, *A&A*, 462, 101
- Chary, R., Becklin, E.E., Evans, A.S., Neugebauer, G., Scoville, N.Z., Matthews, K. & Ressler, M.E. 2000, *ApJ*, 531, 756
- Claussen, M.J., Diamond, P.J., Braatz, J.A., Wilson, A.S. & Henkel, C. 1998, *ApJ*, 500, L129
- de Vaucouleurs, G., de Vaucouleurs, A., Corwin, H.G., Buta, R.J., Paturel, G. & Fouque, P. 1991, *Third Reference Catalog of Bright Galaxies*, (Berlin:Springer Verlag)
- Fullmer, L. & Lonsdale, C. 1989, *Cataloged Galaxies and Quasars Observed in the IRAS Survey, Version 2*, JPL D-1932

- Genzel, R. & Downes, D. 1977, *A&AS*, 30, 145
- Greenhill, L.J. 2004, *New ARev.*, 48, 1079
- Greenhill, L.J., Henkel, C., Becker, R., Wilson, T.L. & Wouterloot, J.G.A. 1995a, *A&A*, 304, 21
- Greenhill, L.J., Jiang, D.R., Moran, J.M., Reid, M.J., Lo, K.Y. & Claussen, M.J. 1995b, *ApJ*, 440, 619
- Greenhill, L.J., Kondratko, P.T., Lovell, J.E.J., Kuiper, T.B.H., Moran, J.M., Jauncey, D.L. & Baines, G.P. 2003, *ApJ*, 582, L11
- Hagiwara, Y., Diamond, P.J. & Miyoshi, M. 2002, *A&A*, 383, 65
- Hagiwara, Y., Diamond, P.J. & Miyoshi, M. 2003, *A&A*, 400, 457
- Henkel, C., Peck, A.B., Tarchi, A., Nagar, N.M., Braatz, J.A., Castangia, P., & Moscadelli, L. 2005, *A&A*, 436, 75
- Herrnstein, J.R., Moran, J.M., Greenhill, L.J., Diamond, P.J., Inoue, M., Nakai, N., Miyoshi, M., Henkel, C. & Riess, A. 1999, *Nature*, 400, 539
- Ho, L.C., Fillipenko, A.V. & Sargent, W.L.W. 1997, *ApJ*, 487, 568
- Hu, W. 2005, in *ASP Conf. Ser. 339, Observing Dark Energy*, ed. S. C. Wolff & T. R. Lauer (San Francisco: ASP), 215
- Humphreys, E.M.L., Reid, M.J., Greenhill, L.J., Moran, J.M. & Argon, A.L., 2008, *ApJ*, in press.
- Kondratko, P.T., Greenhill, L.J. & Moran, J.M. 2006a, *ApJ*, 652, 136
- Kondratko, P.T., Greenhill, L.J., Moran, J.M., Lovell, J.E.J., Kuiper, T.B., Jauncey, D.L. & Kuiper, T.B., Cameron, L.B., Gomez, J.F., Garca-Miro, C., Moll, E., de Gregorio-Monsalvo, I., McCallum, J. & Jimnez-Bailn, E., 2006b, *ApJ*, 638, 100
- Lo, K.Y., 2005, *ARA&A*, 43, 625
- Macri, L.M., Stanek, K.Z., Bersier, D., Greenhill, L.J. & Reid, M.J. 2006, *ApJ*, 652, 1133
- Maoz, E. & McKee, C. 1998, *ApJ*, 494, 218
- Nakai, N, Sato, N. & Yamauchi, A. 2002, *PASJ*, 54, L27

- Peck, A.B., Henkel, C., Ulvestad, J.S., Brunthaler, A., Falcke, H., Elitzur, M., Menten, K.M. & Gallimore, J.F. 2003, ApJ, 590, 149
- Sanders, D.B., Mazzarella, J.M., Kim, D.-C., Surace, J.A. & Soifer, B. T., AJ, 126, 1607
- Spergel, D.N. et al. 2007, ApJS, 170, 377
- Tarchi, A., Henkel, C., Peck, A.B. & Menten, K. 2002, A&A, 389, L39
- Veron-Cetty, M.-P. & Veron, P. 2003, A&A, 412, 399
- Watson, W.D. & Wallin, B.K. 1994, ApJ, 432, L35
- Zhang, J.S., Henkel, C., Kadler, M., Greenhill, L.J., Nagar, N., Wilson, A.S. & Braatz, J.A. 2006, A&A, 450, 933

Table 1: H₂O Masers Detected During the GBT Survey

Source	α_{2000} (h m s)	δ_{2000} (° ' ")	V_{hel}^a (km s ⁻¹)	S_{peak}^b (mJy)	L_{iso}^c (L_{\odot})	Date of Observation
NGC 23	00 09 53.4	+25 55 26	4566 ± 2	51	180	26 Nov 2006
NGC 1106	02 50 40.5	+41 40 17	4337 ± 19	74	8	20 Nov 2005
UGC 3193	04 52 52.6	+03 03 26	4454 ± 10	130	270	20 Nov 2005
UGC 3789	07 19 30.9	+59 21 18	3325 ± 24	134	370	21 Dec 2005
NGC 2989	09 45 25.2	-18 22 26	4146 ± 5	36	40	20 Nov 2005
NGC 3359	10 46 36.8	+63 13 25	1014 ± 1	40	0.7	31 Dec 2005
NGC 4527	12 34 08.5	+02 39 14	1736 ± 1	16	4	14 Apr 2007
NGC 7479	23 04 56.7	+12 19 22	2381 ± 1	138	19	30 Dec 2006

^aHeliocentric recession velocity from the NASA/IPAC Extragalactic Database

^bPeak flux density

^cInferred isotropic luminosity of the maser emission.

Table 2. Galaxies surveyed for water maser emission but not detected.

Source	α_{2000} (h m s)	δ_{2000} (° ' ")	Velocity (km s ⁻¹)	Date	T _{sys} (K)	Time (min)	rms ₁ (mJy)	V ₁ range (km s ⁻¹)	rms ₂ (mJy)	V ₂ range (km s ⁻¹)
NGC 7805	0 01 26.76	+31 26 01.4	4850	2006 Jan 5	43.8	5	6.0	3464 – 6248	5.7	5968 – 8799
NGC 7806	0 01 30.06	+31 26 30.7	4768	2006 Jan 5	42.2	5	5.7	3383 – 6166	5.7	5885 – 8715
NGC 7817	0 03 58.91	+20 45 08.3	2309	2005 Dec 14	42.4	5	6.5	946 – 3684	7.2	3408 – 6192
NGC 7819	0 04 24.54	+31 28 19.3	4958	2006 Jan 5	39.7	5	5.7	3571 – 6357	5.3	6077 – 8910
NGC 1	0 07 15.83	+27 42 29.1	4545	2005 Dec 14	41.1	5	6.6	3162 – 5941	7.7	5661 – 8486
NGC 12	0 08 44.81	+04 36 44.9	3940	2005 Oct 2	60.6	5	8.5	3802 – 6592	9.0	1333 – 4078
NGC 13	0 08 47.73	+33 26 00.0	4808	2006 Oct 30	41.4	5	5.7	3422 – 6206	5.3	5926 – 8755
NGC 9	0 08 54.69	+23 49 01.3	4528	2005 Dec 14	41.8	5	6.0	3145 – 5923	5.9	5644 – 8468
NGC 16	0 09 04.28	+27 43 45.9	3056	2005 Dec 14	42.2	5	5.7	1686 – 4438	5.4	4161 – 6958
NGC 26	0 10 25.86	+25 49 54.6	4589	2005 Dec 14	41.2	5	5.5	3205 – 5985	5.5	5705 – 8531

Note. — Table 2 is published in its entirety in the electronic edition of the *Astrophysical Journal*. A portion is shown here for guidance regarding its form and content. Col (1): Source name. Cols. (2 – 3): RA and Dec (J2000). Col. (4): Recession velocity. Col. (5): Date of observation. Col. (6): System temperature measured from the first spectral window. Col. (7): Integration time. Col. (8): Rms noise measured for the first spectral window, after Hanning smoothing. Col. (9): Velocity range covered by the first window. Col. (10): Rms noise measured for the second window, after Hanning smoothing. Col. (11): Velocity range covered by the second window.

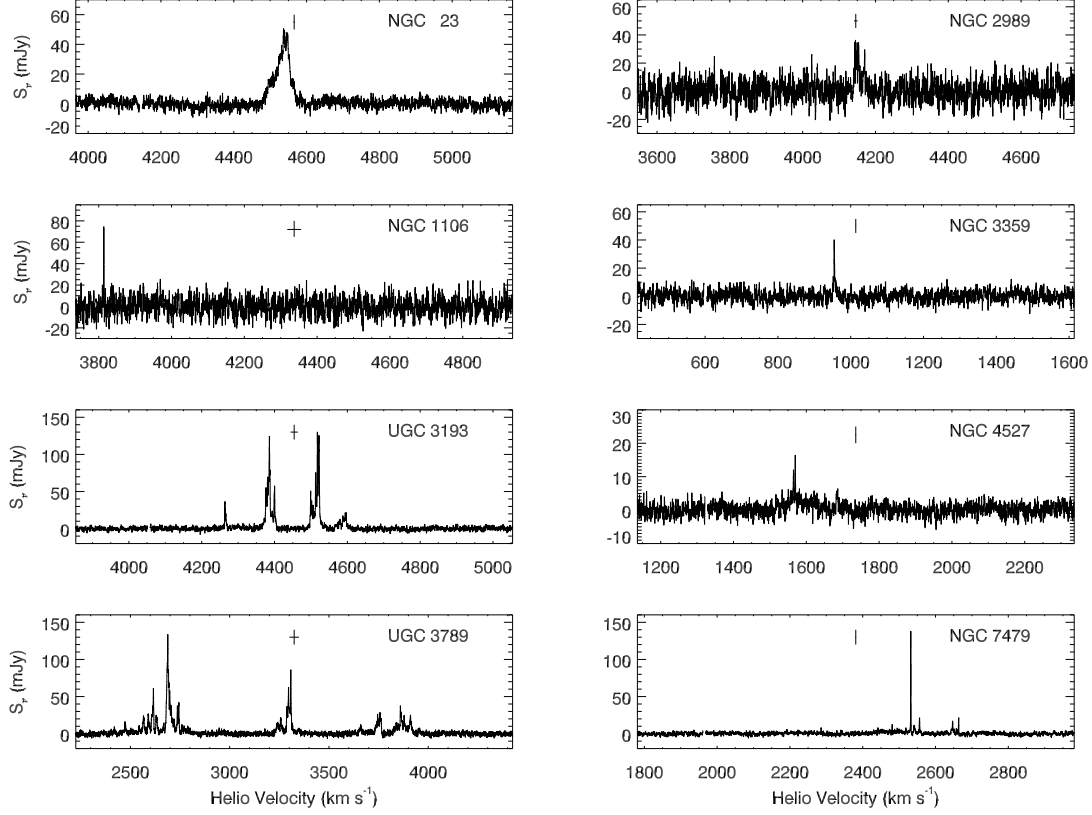


Fig. 1.— Spectra of newly discovered 22 GHz water masers toward the nuclei of 8 galaxies. The vertical line above each spectrum marks the systemic recession velocity of the galaxy and its $\pm 1\sigma$ uncertainty is indicated by the horizontal bar. Each spectrum spans 1200 km s^{-1} except UGC 3789, which covers 2200 km s^{-1} . Velocities are heliocentric and use the optical definition of Doppler shift.

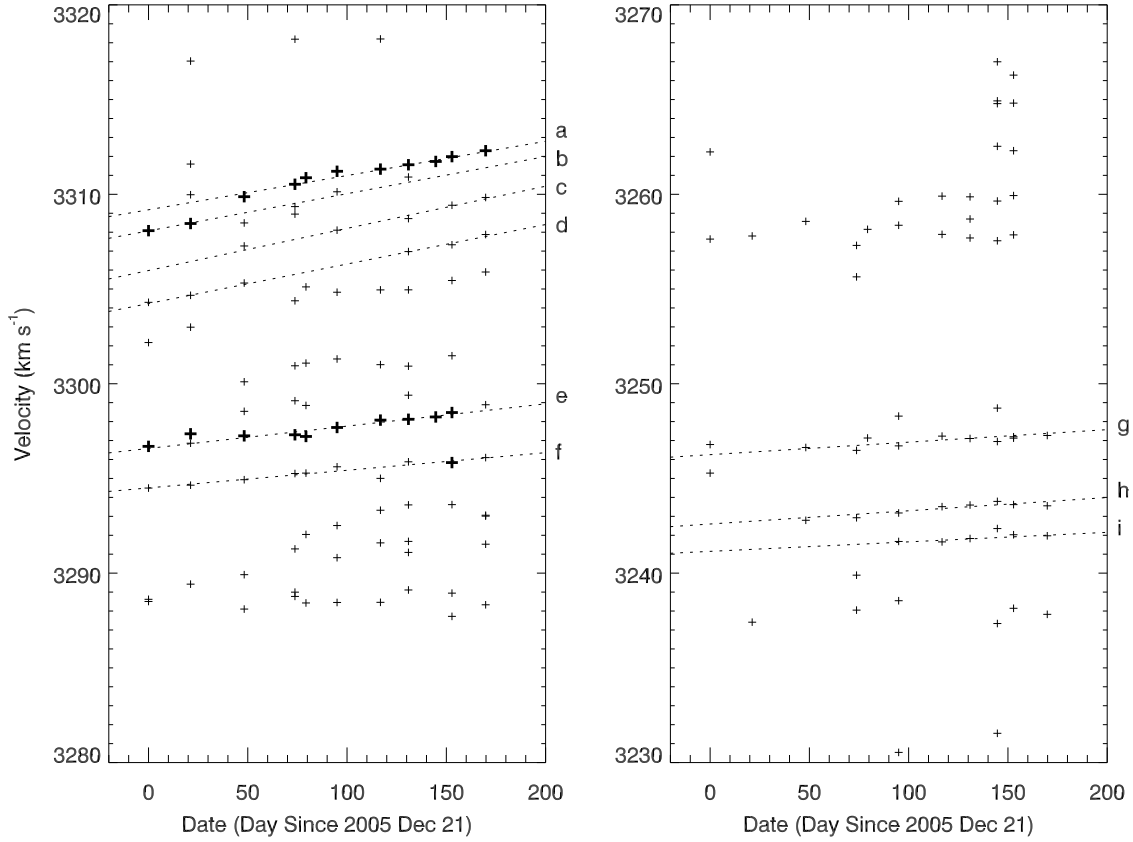


Fig. 2.— The velocities of selected maser components in UGC 3789 are plotted as a function of date of observation, in days since the discovery date of 2005 Dec 21. The bold symbols denote prominent features with fluxes at least 30 mJy above emission at nearby frequencies. Velocities were determined by Gaussian fits. Only narrow components distinguished from the base level of emission were fit, although in several cases we fit multiple Gaussians to model blended features. The accelerations of the emission lines identified by dashed lines, measured by least squares linear fits and listed here in units of $\text{km s}^{-1} \text{yr}^{-1}$, are (a) 6.6 ± 0.1 ; (b) 7.2 ± 0.2 ; (c) 8.1 ± 0.4 ; (d) 7.6 ± 0.2 ; (e) 4.3 ± 0.1 ; (f) 3.4 ± 0.1 ; (g) 2.4 ± 0.2 ; (h) 2.6 ± 0.3 ; and (i) 1.8 ± 0.5 . The identification letters here correspond to the those on the right side of each plot panel.

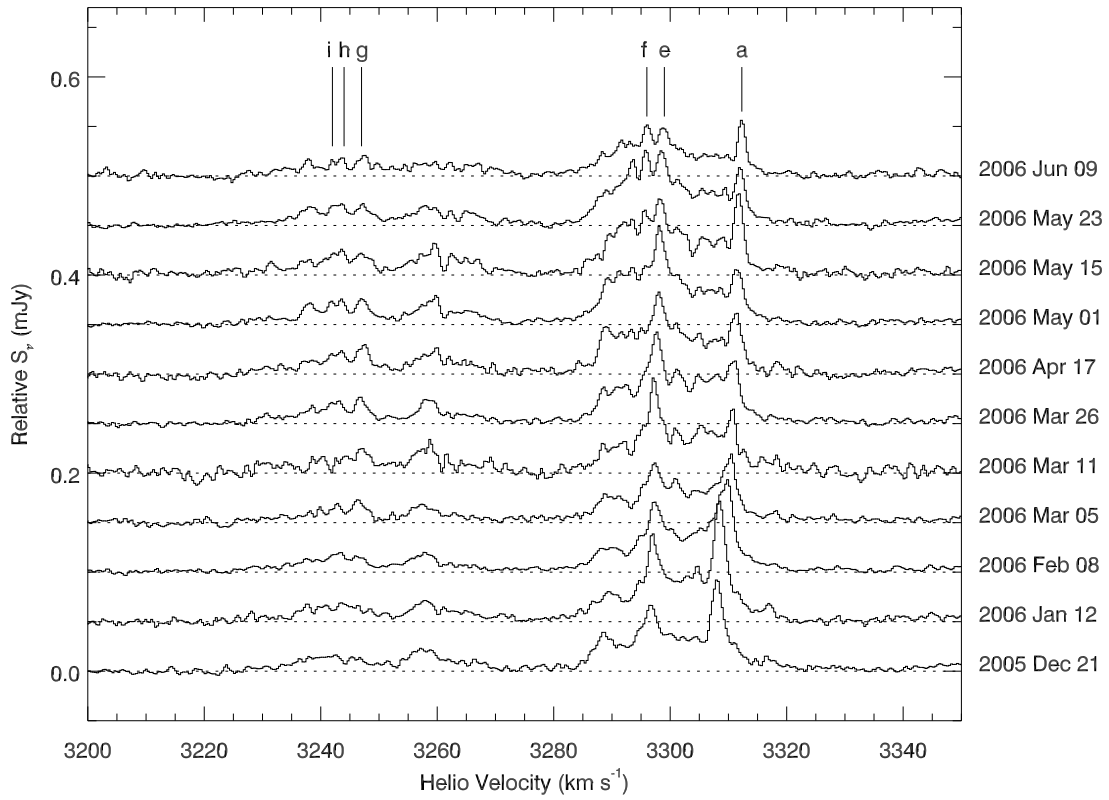


Fig. 3.— Spectra of water maser emission from UGC 3789 near the systemic recession velocity of the galaxy, spanning eleven epochs. The spectra are offset for clarity. The labels at the top of the figure match individual features to those identified in Figure 2.